

Research Article

Synergistic Removal of Bromate and Ibuprofen by Graphene Oxide and TiO₂ Heterostructure Doped with F: Performance and Mechanism

Yan Zhang ¹, Jiarong Li,² and Hongyuan Liu ³

¹Department of Civil Engineering, Zhejiang University, 866 Yuhangtang Rd., Hangzhou 310058, China

²College of Civil Engineering and Architecture, Zhejiang University, 866 Yuhangtang Rd., Hangzhou 310058, China

³College of Civil Engineering and Architecture, Zhejiang University of Technology, 18 Chaowang Rd., Hangzhou 310014, China

Correspondence should be addressed to Hongyuan Liu; lhyzyy@zjut.edu.cn

Received 4 December 2019; Revised 4 February 2020; Accepted 5 February 2020; Published 5 March 2020

Academic Editor: Takuya Tsuzuki

Copyright © 2020 Yan Zhang et al. This is an open access article distributed under the Creative Commons Attribution License, which permits unrestricted use, distribution, and reproduction in any medium, provided the original work is properly cited.

The batch experiments of photocatalytic oxidation-reduction of bromate and ibuprofen (IBP) by graphene oxide (GO) and TiO₂ heterostructure doped with F (FGT) particles were conducted. The performance and mechanism of synergistic removal of bromate and IBP by FGT were discussed. The results show that a demonstrable synergistic effect and excellent removal rate of bromate and IBP by FGT were exhibited. When pH is 5.2 and the dosage of FGT is 0.1 g/L, the reaction rate constants of bromate and IBP increased from 0.0584 min⁻¹ and 0.4188 min⁻¹ to 0.1353 min⁻¹ and 0.4504 min⁻¹, respectively, compared with the degradation of bromate or IBP alone. The reaction of photocatalytic synergistic degradation is appropriately fitted through Langmuir-Hinshelwood first-order kinetics. The mechanism of synergistic removal of bromate and IBP by FGT was discussed. And electrons (e⁻), hydroxyl radical (·OH), and superoxide radical (·O₂⁻) are the main active species. The electrons play a main role in the bromate reduction, and bromine is the only reduction product, while the oxidation of IBP is the result of ·OH and ·O₂⁻, and ·OH plays a key role. The recombination of electrons and holes is inhibited by simultaneous consumption of bromate and IBP, which makes full use of the redox properties of FGT and plays a synergistic role in the removal of pollutants. The results indicate that photocatalytic oxidation-reduction by FGT is a promising, efficient, and environmental-friendly method for synchronous removal of combined pollution in water.

1. Introduction

With the development of industry and agriculture, the complex characteristics of water pollution are becoming more and more prominent. Advanced oxidation processes (AOPs) have been shown effective technologies to destroy recalcitrant contaminants in the aqueous phase. And, due to its advantages of high efficiency, good photochemical stability, nontoxicity, and low cost, TiO₂ photocatalysis has been proved to be one of the most promising environmental-friendly technologies for the decomposition of environmental pollutants, and it has been widely studied in water treatment and air pollution control [1–3].

However, the photocatalytic activity of TiO₂ is limited by band gap and the recombination of photogenerated electron-

hole pairs. The performance of TiO₂ photocatalysts can be obviously enhanced through appropriate modification, and co-doped TiO₂ usually exhibits better results of pollutants removal than singly doped TiO₂ [4, 5]. In our previous work, a photocatalyst of graphene oxide (GO) and TiO₂ heterostructure doped with F (FGT) was synthesized, which exhibited a commendable reduction performance of bromate [6]. Over 90% of 100 μg/L bromate could be removed with a 0.05 g/L dosage of F_{1.0}G_{0.1}T in 15 minutes under UV irradiation at intensity of 26 μW/cm² and pH of 5.2. Graphene oxide is used to narrow the band gap and accelerate electron migration, which exists in the form of Ti-C and works as an electron-transporting bridge and electron sink. And HF is introduced to TiO₂ as the crystal control agent, and it is effective at suppressing the recombination of photogenerated

electron-hole pairs, mainly due to the formation of a {001} crystal [6]. The hole and electron produced by the light irradiation of TiO_2 have strong oxidation ability and reduction ability, respectively [7]. Therefore, with the electron-hole synergy, the coexistence of contaminants as the electron acceptor and the electron donor may be removed at the same time, and a synergy will occur, which is beneficial to improve the removal rates for both reducing substances and oxidizing substances.

However, to the best of our knowledge, few studies on the synergistic removal of contaminants by photogenerated electrons and holes over TiO_2 photocatalysts can be found. Ibuprofen (IBP), a typical kind of pharmaceutical and personal care products (PPCPs), is a widely used as nonsteroidal anti-inflammatory (NSAID) drug for pain relief. Due to the low removal rate of PPCPs by traditional sewage treatment process [8, 9], IBP cannot be degraded completely and discharged into the environment and thus have been frequently detected in surface water, groundwater, and drinking water [10, 11]. It is considered to an emerging low persistent organic pollutant because of its stable, difficult to volatilize, long half-life, and good migration in aquatic environment [12]. Therefore, IBP and bromate as a typical electron donor and electron acceptor, respectively, were chosen in this work; the performance of FGT for simultaneous removal of bromate and IBP was investigated to verify the synergistic reaction; the effects of initial concentration and the dosage of FGT, pH, and HA on synergistic removal of bromate and IBP were explored; and the function of active species and the mechanism of photocatalytic synergistic removal of bromate and IBP by FGT were also discussed. The goal of this work is to explore the performance and reaction mechanism of synergistic redox of FGT and provide a promising, efficient, and environmental-friendly method for synchronous removal of combined pollution in water.

2. Experimental Section

2.1. Materials. Ethyl alcohol ($\text{C}_2\text{H}_5\text{OH}$), sodium bromate (NaBrO_3), hydrofluoric acid (HF), tert-butanol (TBA), and benzoquinone (BQ) were obtained from the Sinopharm Chemical Reagent (China). The benchmark standard TiO_2 (P25, 99.99%) and graphene oxide (GO, 99.99%) were obtained from Evonik Degussa Specialty Chemicals Co. Ltd (China) and Nanjing Xianfeng Nano-Mstar Technology Ltd (China), respectively. The 5,5-dimethyl-1-pyrrolidine N-oxide (DMPO), IBP (99.9%), and ethylenediaminetetraacetic acid disodium salt dihydrate (EDTA-2Na) were purchased from Aladdin (China). The dimethyl sulfoxide (DMSO) was purchased from Genom (China). All reagents used were of analytical grade and prepared in deionized (DI) water with a resistance of 18.0 M Ω .

2.2. Synthesis and Characterization of Photocatalyst. The FGT photocatalysts were synthesized via a one-step hydrothermal method, with HF as the crystal control agent and GO to accelerate electron migration. GO, P25, and HF were successively introduced into $\text{C}_2\text{H}_5\text{OH}$, then the suspension

was transferred into a Teflon-sealed autoclave and maintained at 180°C for 24 hours, finally washed and dried for future use.

The morphology of the synthesized FGT was characterized using an FEG650 field emission scanning electron microscope (FESEM, FEI, China) and an H-9500 transmission electron microscope (TEM, Hitachi, Japan). The surface compositions and binding energies of the samples were determined using an Escalab X-ray photoelectron spectroscopy (XPS, VG, UK). The results [6] show that size of the composite varies in the range of 10 to 35 nm, and the average dimension is 23 nm; in addition to the spherical particles, cuboid morphologies with {001} and {101} surface can be observed. Furthermore, the result of XPS technique reveals that F1s can be found at approximately 685.3 eV in the FGT, signifying successful F-loading. Meanwhile, XPS of C1s was able to further resolve a weak signal at 283.5 eV that originated from the formation of Ti-C bonds. This peak-fitting result illustrated the successfully doping of GO on the TiO_2 . More details can be seen in Zhang et al. [6].

It can be found that $\text{F}_{1.0}\text{G}_{0.1}\text{T}$ shows the best bromate removal rate under the same conditions, where 1.0 is the mass ratio of HF: P25 (%), and 0.1 is the mass ratio of GO: P25 (%). Thus, unless otherwise specified, the experiments in this study were carried out with $\text{F}_{1.0}\text{G}_{0.1}\text{T}$ that briefly expressed as FGT.

2.3. Batch Experiments. A 500 mL double-glazing bottle placed in a sealed black box was used as a reactor, and a 10 W low-pressure Hg lamp (primary output 254 nm, intensity 26 $\mu\text{W}/\text{cm}^2$) was immersed in the suspension as UV light sources, protected by quartz glass. The batch experiments were carried out under constant temperature and atmospheric pressure conditions. Prior to the experiments, a predetermined concentration of bromate and IBP solution was filled in the reactor; then, a predetermined quantity of FGT was added and suspended in the solution using a magnetic stirrer. Where required, the initial pH was adjusted by addition of appropriate amounts of HCl (0.1 M) or NaOH (0.1 M), and no buffer was added during the experiments. Unless otherwise specified, the experiments were conducted with FGT, pH, temperature, and initial concentration of 0.05 g/L, 5.2 ± 0.2 , 293 K, and 100 $\mu\text{g}/\text{L}$, respectively. All experiments were performed in triplicate.

2.4. Analysis Methods. Samples were periodically taken from the suspension to analyze the concentrations of bromate and IBP. Bromate was analyzed with an Ion Chromatograph (Dionex ICS2000), while IBP was determined by a high-performance liquid chromatography (Agilent 1200). The pH was periodically monitored with an Orion 3-star pH analyzer. The free radicals were measured by electron paramagnetic resonance (EPR), using DMPO as a spin-trapping agent, deionized water and DMSO as solvent for the detection of hydroxyl radical and superoxide radical, respectively.

3. Results and Discussion

3.1. Photocatalytic Properties. The optimal dosage of 0.05 g/L FGT has been shown an excellent reduction effect on bromate alone in our previous work [6]. Based on this, 0.1 g/L FGT was initially used to evaluate the photocatalytic activity of FGT in water polluted by bromate and IBP. The results are shown in Figure 1. It was found from Figure 1(a) that both bromate and IBP can be fully removed with a 0.1 g/L dosage of FGT composite in the coexisting system in 30 min under UV-light irradiation. Moreover, bromate and IBP removal rates exhibited higher in the bromate and IBP coexisting solution system than those in bromate or IBP alone solution; the coexisting IBP can significantly improve bromate removal under the experimental conditions.

In order to further illustrate the interaction between bromate and IBP in the coexisting system under FGT photocatalysis, the kinetic behaviors were discussed. All reactions were appropriately fitted through Langmuir-Hinshelwood first-order kinetics, $\ln(C_0/C) = kt$, where k is the apparent reaction rate constant, C_0 is the initial concentration of reactant, and C is the concentration of reactant at the time. The variations in $\ln(C_0/C)$ as a function of reaction time are given in Figure 1(b), and the calculated apparent rate constant k is shown in Table 1. Compared with the degradation of bromate or IBP alone, the rate constants of bromate and IBP increased from 0.0584 min^{-1} and 0.4188 min^{-1} to 0.1353 min^{-1} and 0.4504 min^{-1} , respectively, obviously increased in the coexisting system.

It suggests that FGT is an efficient photocatalyst for simultaneous oxidation and reduction, and the substances of coexisting system play a synergistic role in their removal rates.

3.2. Effect of Different Factors on Degradation

3.2.1. Photocatalyst Dosage. Batch experiments of simultaneous redox of IBP and bromate at different FGT dosages were performed; the results are shown in Figure 2. The removal rates of bromate and IBP increased with the FGT dosage increase from 0.025 to 0.1 g/L. Although an increase in the photocatalyst dosage improved the removal efficiency of IBP, the removal rate had no distinct difference when the photocatalyst dosage increased from 0.05 to 0.1 g/L. This can be explained that with an increase in the photocatalyst dosage, the catalytic active species effective for the photocatalytic redox reaction were increased, thereby resulting an increase in removal rate. However, when the dosage of catalyst reached a certain value, the light irradiation was hindered and reflected by the excessive catalyst. Therefore, the dosage of 0.05 g/L was used for further studies.

3.2.2. Initial Concentration. The initial concentration of the contaminant is an important parameter in photocatalysis. The interaction between the initial concentrations of the two contaminants in the coexisting solution was explored. As shown in Figure 3(a), the lower initial BrO_3^- concentration, the higher removal rate of BrO_3^- was achieved when the initial IBP concentration is fixed at 0.1 mg/L in the coexisting solution, but the result was opposite when the

initial IBP concentration is fixed at 1.0 mg/L. The removal rate of IBP decreased with an increase of initial IBP concentration when the initial BrO_3^- concentration is constant (Figure 3(b)).

This is due to the fact that the active sites and the amount of photons produced by the catalyst are constant with the same dosage of the catalyst, and the amount of photons obtained by the unit molecule decreases with the increase of initial concentration [13], which is not conducive to the process of photolysis. However, when the initial concentration of IBP is too high in the coexisting system, the possibility of bromate (with an excessively low initial concentration) approaching the surface of FGT was lower than that with higher initial concentrations [14], then leading to the lower removal rate [15]. Therefore, unless otherwise specified, the initial bromate and IBP concentrations of $100 \mu\text{g/L}$ were selected in this work.

3.2.3. pH. Figure 4 shows the removal rates of BrO_3^- and IBP in coexisting solution at different pH. The degradation of BrO_3^- and IBP in coexisting solution declined when pH increased from 2.5 to 9.0. It indicates that the degradation of the coexisting solution is obviously pH dependent. It can be seen that the removal rate was higher under acidic condition than that under neutral or alkaline condition.

This is because BrO_3^- is negative charged, IBP is a weak acid, which has a carboxyl group ($4.52 \leq \text{pKa} \leq 4.9$) [16], while the isoelectric point of FGT measured by a laser particle size analyzer is 6.0 [6]. In acidic solution ($\text{pH} \leq 4.9$), the surface of FGT would be electropositive; negatively charged BrO_3^- and electrically neutral IBP existed in the form of molecule are easily adsorbed. This is beneficial to the subsequent photoreaction, so that better photocatalytic removal efficiencies can be obtained. However, in the solution of $\text{pH} > 4.9$, the surface of FGT would be electronegative, IBP is electronegative due to ionization, and less BrO_3^- and IBP adsorbed on FGT. In addition, several studies have shown that high concentrations of OH^- enabled CO_2 to enter into the solution; CO_3^{2-} was produced consequently, which is a radical scavenger [17]. Therefore, an increase of pH value leads to a decrease in the removal efficiency, as illustrated in Figure 4.

3.2.4. HA. Humic acid is a typical representative of dissolved organic matter (DOM); therefore, the effect of HA on the photocatalytic removal of bromate and IBP coexisting solution was studied. The results are shown in Figure 5. It can be seen that, when the HA added in the solution, the removal rate of bromate decreased, while the removal of IBP improved.

Some studies have shown that HA is easily adsorbed on the surface of the catalyst, which hinders the absorption of light [18]. As a result, the removal ability of bromate reduced to a certain degree. However, the concentration of HA changed from 2.5 to 10.0 mg/L, and the removal efficiency had no distinct difference in this work.

The degradation rate of IBP increased with the HA concentration increase from 1 to 5 mg/L. However, while the HA concentration further increased from 5 to 10 mg/L, the degradation rate of IBP shows no further increase but

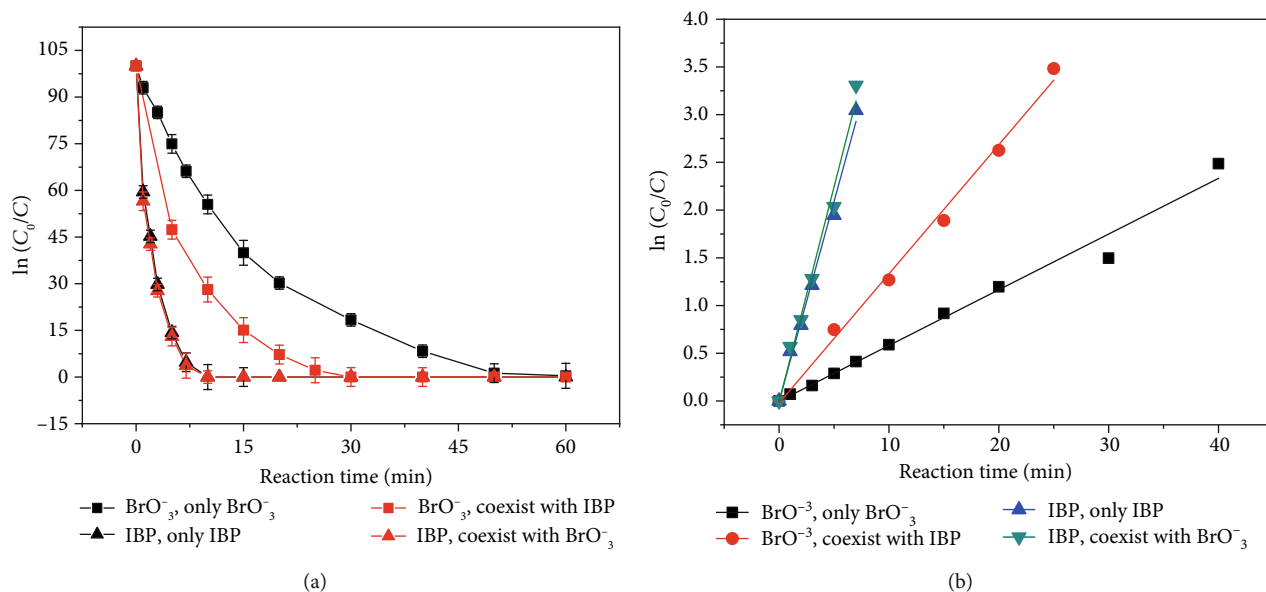


FIGURE 1: (a) Removal efficiencies; (b) reaction kinetics of the photocatalytic degradation by FGT of the coexisting solution of bromate and IBP. $[\text{BrO}_3^-]_0 = 100 \mu\text{g/L}$, $[\text{IBP}]_0 = 100 \mu\text{g/L}$, $[\text{FGT}] = 0.1 \text{ g/L}$, $\text{pH}_0 = 5.2 \pm 0.2$.

TABLE 1: Apparent rate constants for photodegradation of the different reaction system.

Reaction system	Bromate (alone)	Bromate (coexisting IBP)	IBP (alone)	IBP (coexisting bromate)
$k \text{ (min}^{-1}\text{)}$	0.0584	0.1353	0.4188	0.4504

decrease, as shown in Figure 5(b). This is consistent with the literatures [19, 20]. This may be due to excited triplet state of HA ($^3\text{HA}^*$) induced under UV-light radiation. On the one hand, the excitation energy is transferred directly to the organic molecules to form IBP^* and make the IBP photolysis directly [21]. On the other hand, the formation of reactive species by the reaction of $^3\text{HA}^*$ with dissolved oxygen make the IBP photolysis indirectly [22, 23]. In addition, due to the competition for photons and reactive oxygen radicals between HA and IBP under high concentration of HA [18], the inhibition effect on IBP degradation enhances, thereby results a slight decrease in removal rate with the HA concentration increases from 5 to 10 mg/L.

3.3. Mechanism of the Photocatalytic Degradation

3.3.1. Action of Active Species. It has been reported that $\cdot\text{OH}$, O_2^- , and h^+ were the main active species in the photocatalytic degradation [24]. To clearly investigate the main types and roles of active species involved in the photocatalysis process, the scavenger experiments were performed. TBA, BQ, and EDTA-2Na were chosen as the $\cdot\text{OH}$, O_2^- , and h^+ scavengers, respectively, and the concentrations of them in the solution were 0.1 mol/L, 0.1 mmol/L, and 0.1 mmol/L, respectively [25, 26].

As demonstrated in Figure 6, the degradation rate constant of bromate increased from 0.0655 min^{-1} to 0.1614 min^{-1} with the addition of EDTA-2Na scavenger, namely, the

degradation rate of bromate significantly increased. However, the degradation rates decreased slightly while TBA and BQ scavengers added. The results indicate that the EDTA-2Na promote the bromate removal, while the TBA and BQ inhibit it. This may be explained that the probability of electron-hole recombination decreases after h^+ is trapped, which makes an increase in electron concentration, and is beneficial to the bromate removal. In addition, IBP is the main h^+ consumer in the coexisting system, the removal rate of IBP decreases after the $\cdot\text{OH}$ and O_2^- were removed, the h^+ consumption decreases, and the probability of electron-hole recombination increases, which leads to a decrease in the removal rate of bromate. Therefore, it can be considered that e^- is the dominant active species in the bromate removal.

In the process of photocatalytic degradation of IBP, the degradation rate constant of IBP significantly decreased from 0.3294 min^{-1} to 0.0316 , 0.0632 , and 0.0475 min^{-1} with TBA, BQ, and EDTA-2Na added, respectively. The results indicate that $\cdot\text{OH}$, O_2^- , and h^+ do occur in the reaction process and play a role in the photocatalytic degradation of IBP. And the calculated contribution rates of $\cdot\text{OH}$, O_2^- , and h^+ to IBP degradation were 90.4%, 80.8%, and 85.6%, respectively [13]. The total contribution rates of $\cdot\text{OH}$ and O_2^- are more than 100%, indicating that there is a transformation between them. It is speculated that in the process of photocatalytic oxidation of IBP, besides the reaction of h^+ and H_2O , the production of $\cdot\text{OH}$ can be further transformed from the

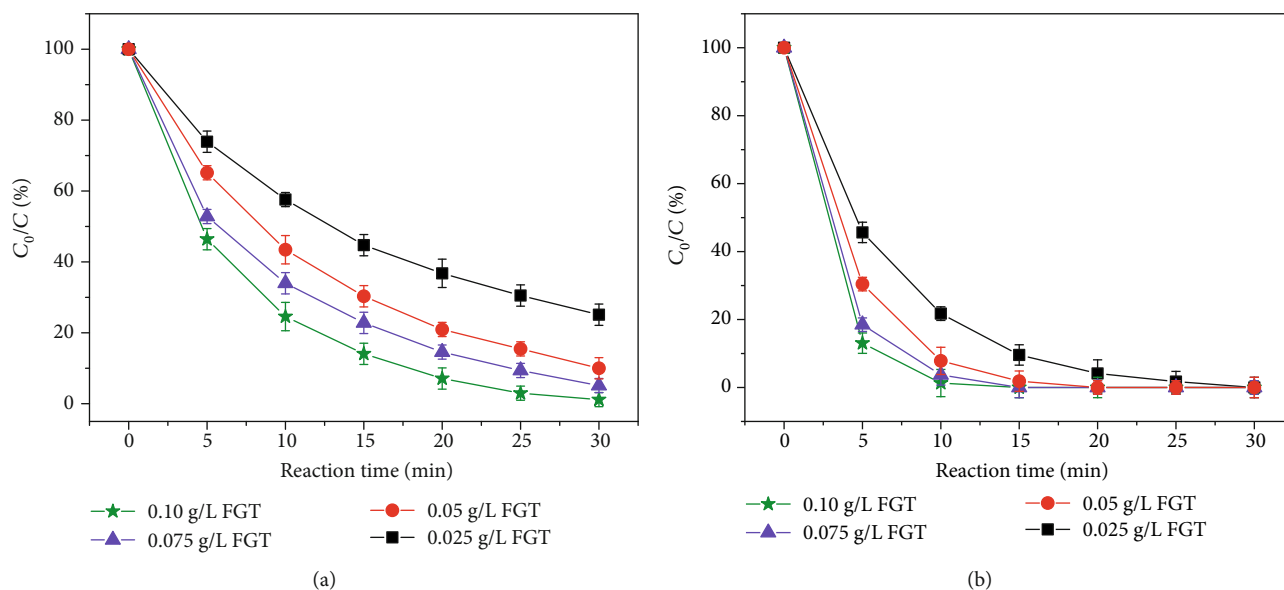


FIGURE 2: Effect of photocatalyst dosage on the photocatalytic (a) reduction of bromate, (b) oxidation of IBP, in the coexisting solution of bromate and IBP by FGT. $[\text{BrO}_3^-]_0 = 100 \mu\text{g/L}$, $[\text{IBP}]_0 = 100 \mu\text{g/L}$, $\text{pH}_0 = 5.2 \pm 0.2$.

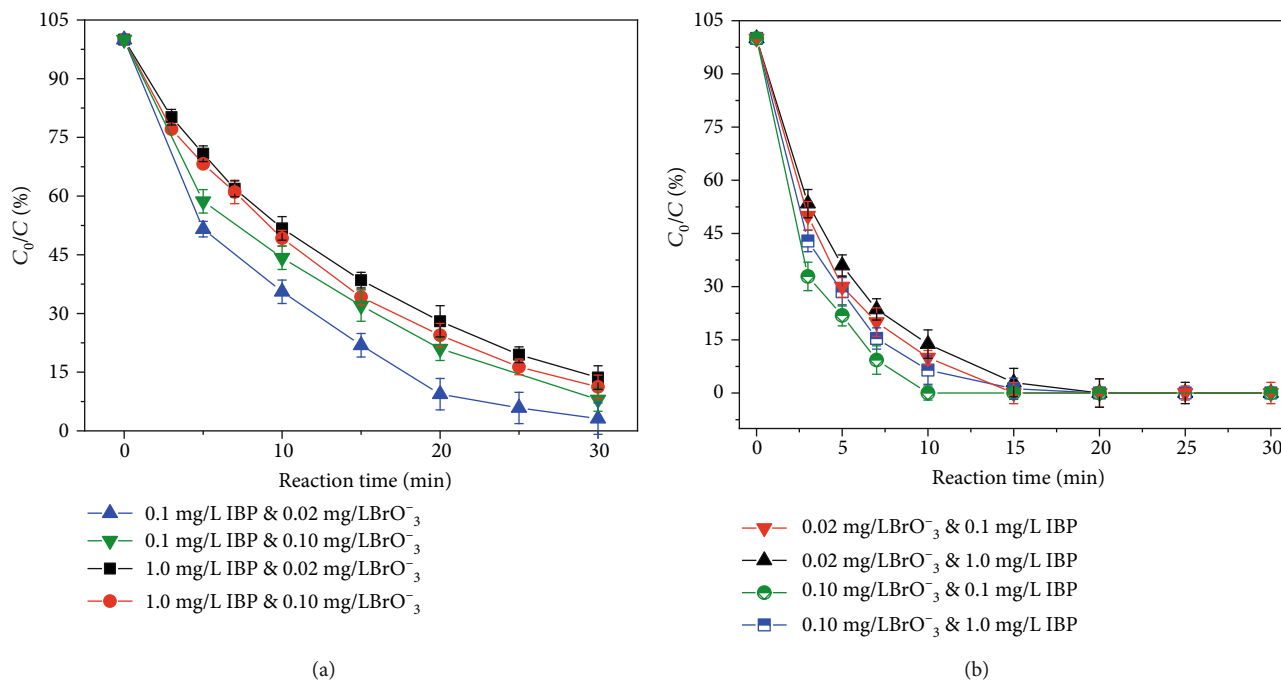


FIGURE 3: Effect of initial concentration on the photocatalytic (a) reduction of bromate, (b) oxidation of IBP, in the coexisting solution of bromate and IBP by FGT. $[\text{FGT}] = 0.05 \text{ g/L}$, $\text{pH}_0 = 5.2 \pm 0.2$.

$\cdot\text{O}_2^-$ produced by e^- . The results reveal that both the $\cdot\text{OH}$ and the $\cdot\text{O}_2^-$ occur and participate in the IBP degradation process, and $\cdot\text{OH}$ plays a key role.

3.3.2. Free Radical Identification. To further confirm the active species, the EPR/DMPO spin-trapping experiments were carried out under UV light irradiation [26]. The results

reveal that no DMPO- $\cdot\text{OH}$ or DMPO- $\cdot\text{O}_2^-$ spin adducts were detected before irradiation, while after irradiation, characteristic peaks of DMPO- $\cdot\text{OH}$ were obviously observed in the FGT/DMPO system as shown in Figure 7(a).

As reported, $\cdot\text{O}_2^-$ is unstable in aqueous solution and is easily transformed to $\cdot\text{OH}$, and the reaction rate constant of DMPO with $\cdot\text{OH}$ is much larger than that with $\cdot\text{O}_2^-$ [27].

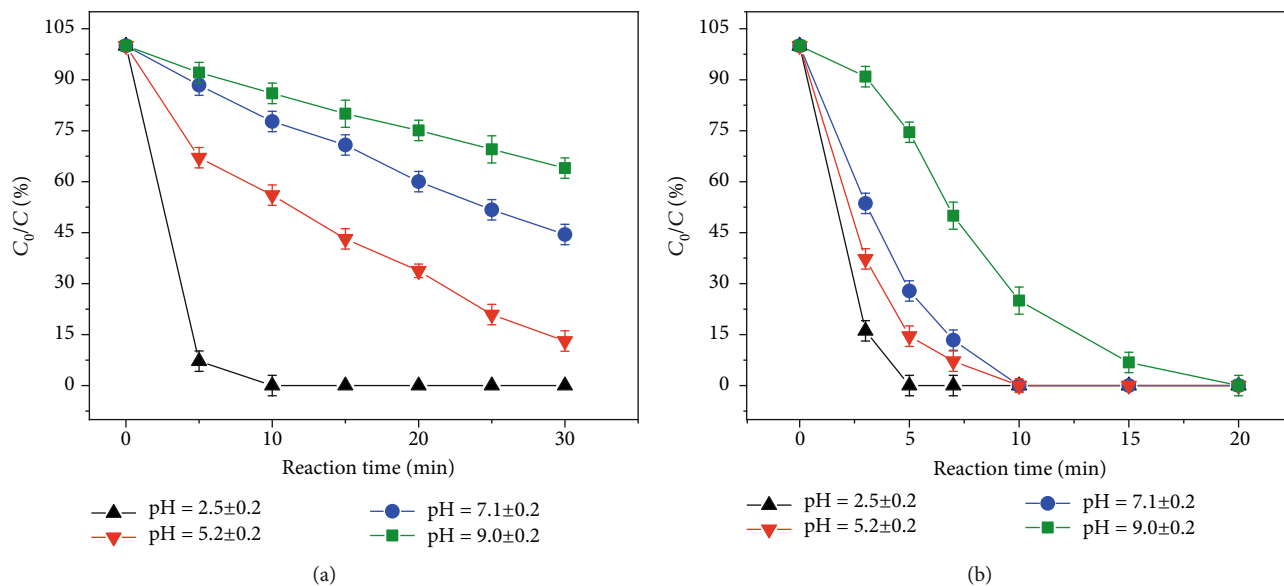


FIGURE 4: Effect of pH on the photocatalytic (a) reduction of bromate, (b) oxidation of IBP, in the coexisting solution of bromate and IBP by FGT. $[\text{BrO}_3^-]_0 = 100 \mu\text{g/L}$, $[\text{IBP}]_0 = 100 \mu\text{g/L}$, $[\text{FGT}] = 0.05 \text{ g/L}$.

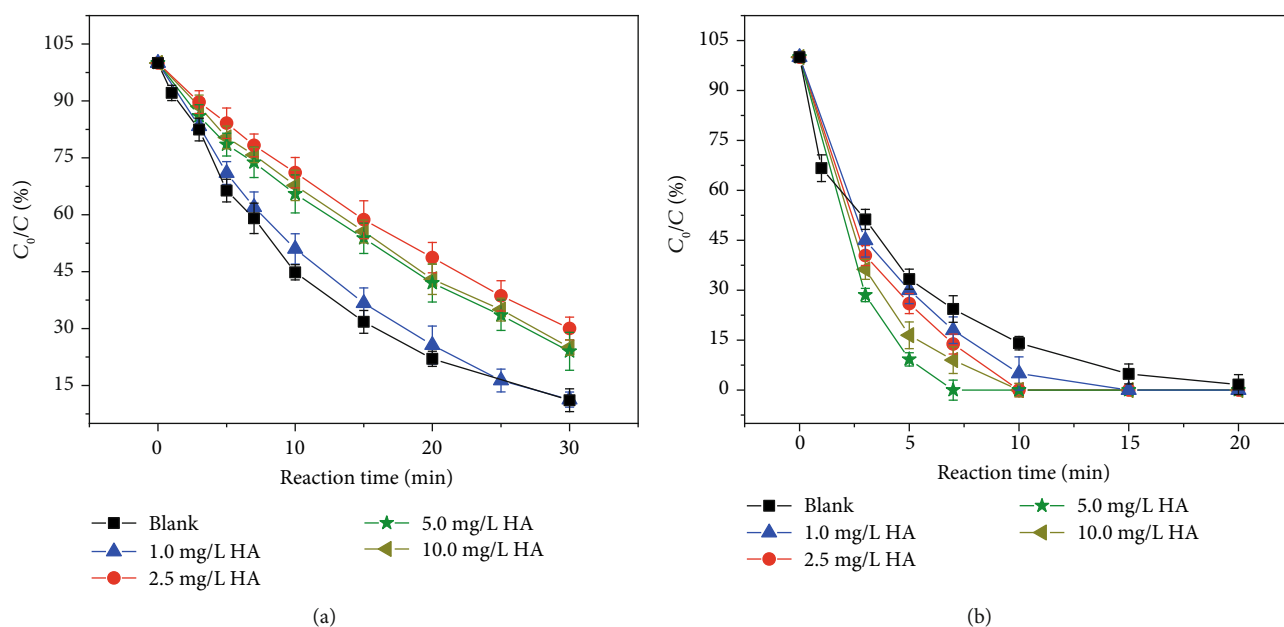


FIGURE 5: Photocatalytic removal rates of (a) bromate, (b) IBP in the coexisting solution of bromate and IBP by FGT under different HA concentrations. $[\text{BrO}_3^-]_0 = 100 \mu\text{g/L}$, $[\text{IBP}]_0 = 100 \mu\text{g/L}$, $[\text{FGT}] = 0.05 \text{ g/L}$, $\text{pH}_0 = 5.2 \pm 0.2$.

So, in order to further verify the generation of $\cdot\text{O}_2^-$ in the system, a polar aprotic solvent DMSO was used as dissolvant instead of deionized water [28], and the results are illustrated in Figure 7(b). It shows that characteristic peaks of $\cdot\text{O}_2^-$ can be observed when DMSO was used as dissolvant instead of deionized water, revealing that $\cdot\text{O}_2^-$ occur and participate in the IBP degradation process.

Above all, FGT is irradiated by ultraviolet light to produce electron and holes (h^+). Most of the e^- is used for the reduction

of bromate, others to form the $\cdot\text{O}_2^-$. While the h^+ is used to form the $\cdot\text{OH}$. The $\cdot\text{OH}$ and $\cdot\text{O}_2^-$ are used for the oxidation of IBP, and $\cdot\text{OH}$ plays a key role. Moreover, the order of the contribution rates is as follows: $\cdot\text{OH}$ formed by h^+ $>$ $\cdot\text{O}_2^-$ $>$ $\cdot\text{OH}$ transformed by $\cdot\text{O}_2^-$. Combined with previous characterization of FGT [6], the proposed mechanism of synergistic removal of bromate and IBP by FGT is shown in Figure 8.

FGT possesses cuboid morphologies with $\{001\}$ and $\{101\}$ facets in addition to spherical particles [6]. Photoinduced

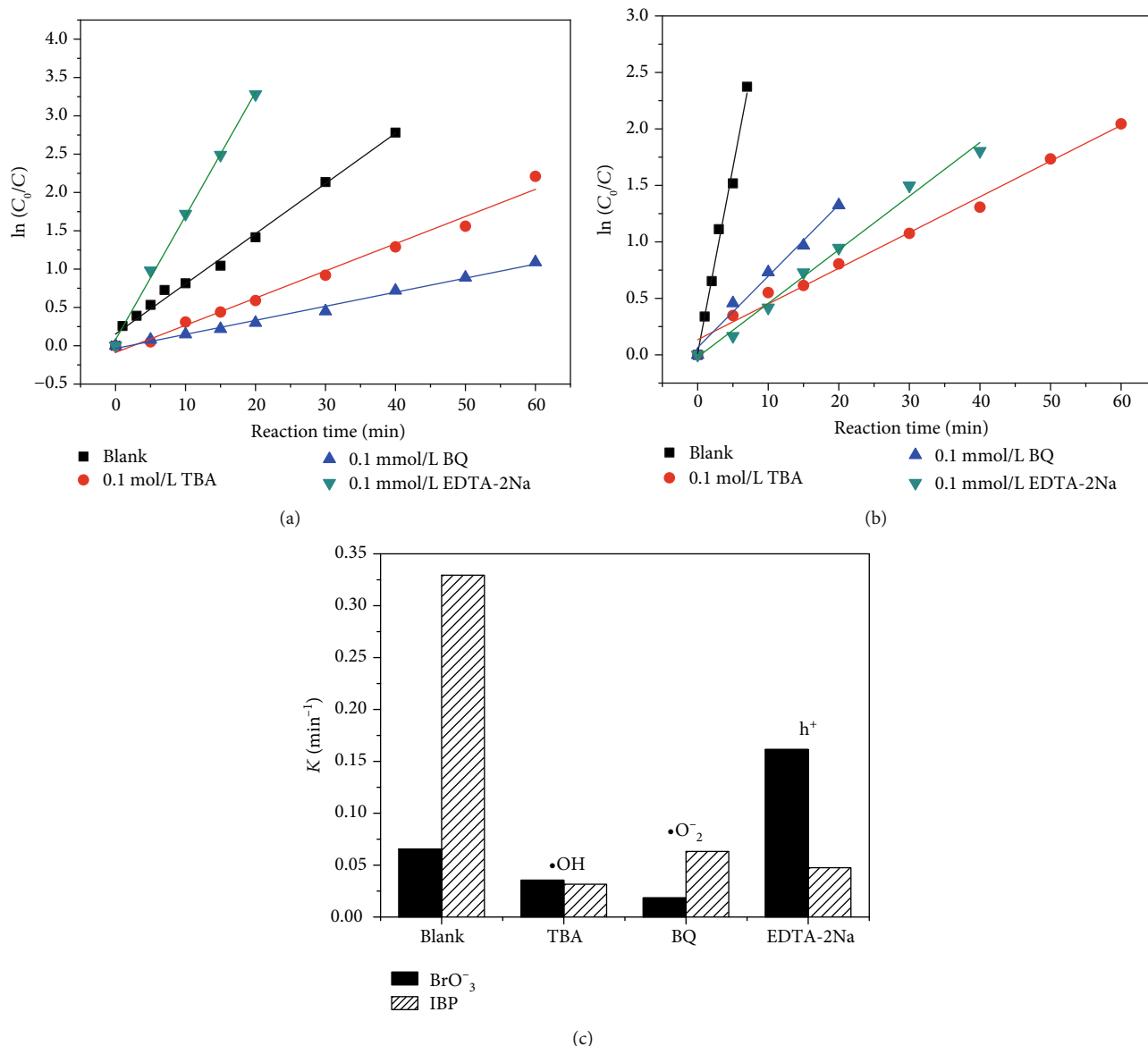


FIGURE 6: Effect of scavenger added on degradation kinetics of (a) bromate, (b) IBP in the coexisting solution. (c) Effect of scavenger added on apparent rate constants k . $[\text{BrO}_3^-]_0 = 100 \mu\text{g/L}$, $[\text{IBP}]_0 = 100 \mu\text{g/L}$, $[\text{FGT}] = 0.05 \text{ g/L}$, $\text{pH}_0 = 5.2 \pm 0.2$.

electrons will be more inclined to migrate to {101} surfaces than those with low potential to participate in bromate reduction, and photogenerated holes are gathered at the {001} crystal surface to take part in the oxidation reaction. Therefore, the formation of a cuboid morphology helps to promote the migration of electrons and to inhibit the recombination of photogenerated electron-hole pairs. This is one of the main aspects of the enhanced photocatalytic activity that allows anisotropic semiconducting crystals to perform better than spherical particles.

Furthermore, the results of UV-vis DRS shows FGT obviously affects the light absorption characteristics of photocatalysts, and the band gap energy of FGT is further red-shifted from 2.98 eV to 2.93 eV (Figure 8). The narrower band gap will eventually lead to bigger density of photogenerated

electron on the conduction band to participate in the pollutants removal and then promote the removal of pollutants under UV photocatalysis.

Based on these characteristics and their synergistic effects, FGT presents excellent photocatalytic activity and stability for bromate and IBP removal under weak UV light irradiation.

4. Conclusion

In this paper, the performance and mechanism of synergistic removal of bromate and IBP by FGT were investigated. Evaluation of the main types and roles of active species was discussed in light of scavenger experiments and free radical identification. The main conclusions generated from this study are as follows: (1) FGT exhibits a remarkable synergistic

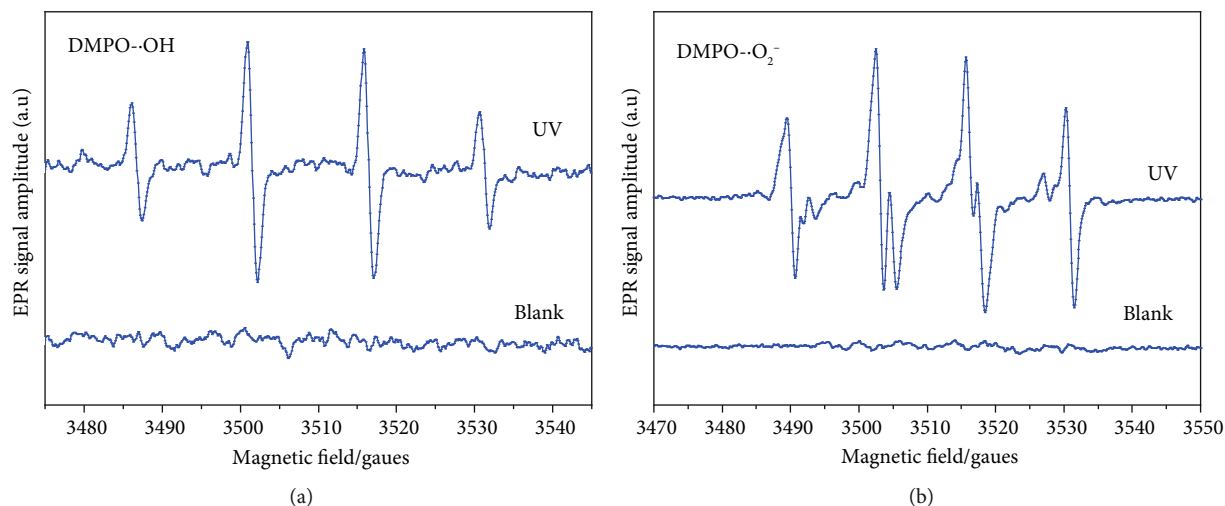


FIGURE 7: DMPO spin-trapping EPR spectra in the presence of FGT and DMPO: (a) deionized water as dissolvant, (b) DMSO as dissolvant.

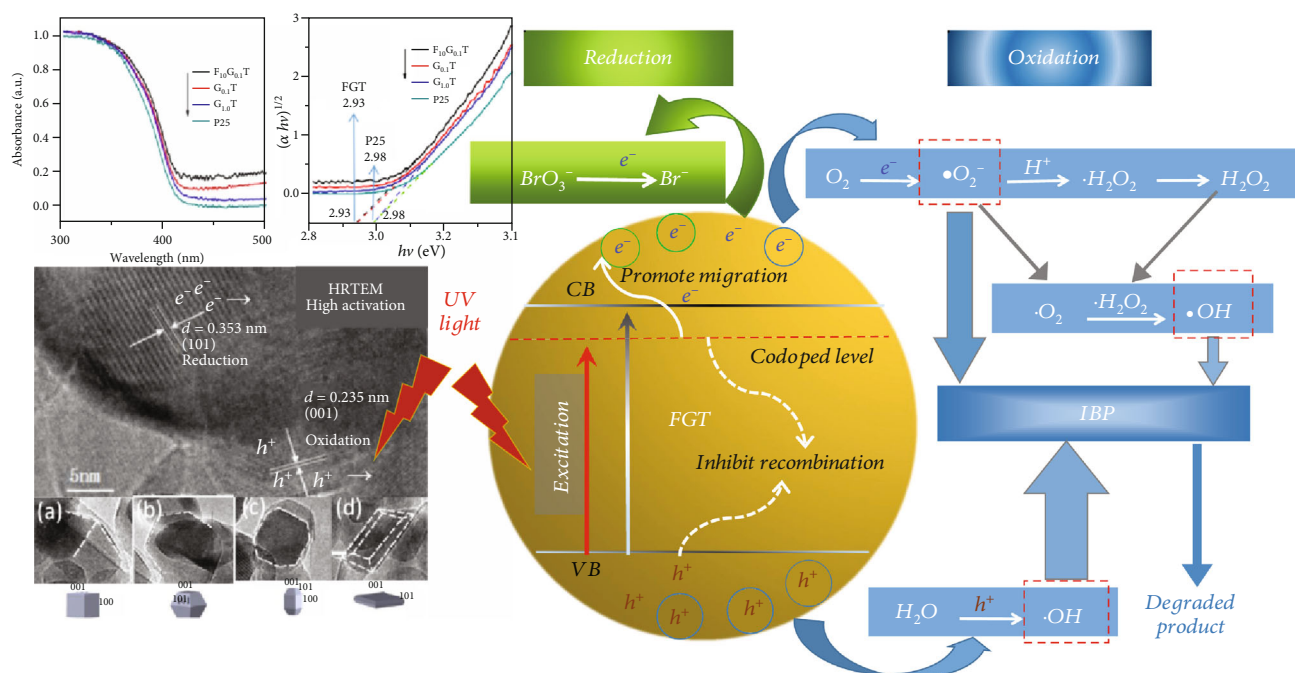


FIGURE 8: Mechanism of synergistic removal of bromate and IBP by FGT.

removal effect on the bromate and IBP. Compared with the degradation of bromate or IBP alone, the rate constants of bromate and IBP increased from 0.0584 min^{-1} and 0.4188 min^{-1} to 0.1353 min^{-1} and 0.4504 min^{-1} , respectively. (2) The synergetic removal of bromate and IBP by FGT fit a first-order reaction kinetics. The e^- , $\cdot\text{OH}$, and $\cdot\text{O}_2^-$ are the primary active species involved in the photocatalytic degradation of bromate and IBP. e^- is the main active substance in the bromate removal, while $\cdot\text{OH}$ is the main active substance for the IBP removal.

Data Availability

The datasets generated during and/or analyzed during the current study are available from the corresponding author on reasonable request.

Conflicts of Interest

The authors declare that they have no conflicts of interest.

Acknowledgments

This research was supported by the National Science and Technology Major Project of China-Water Pollution Control and Treatment (2017ZX07201004).

References

- [1] Y. Song, N. Li, D. Chen et al., "N-doped and CdSe-Sensitized 3D-ordered TiO₂ Inverse opal films for synergistically enhanced photocatalytic performance," *ACS Sustainable Chemistry & Engineering*, vol. 6, no. 3, pp. 4000–4007, 2018.
- [2] D. Awfa, M. Ateia, M. Fujii, M. S. Johnson, and C. Yoshimura, "Photodegradation of pharmaceuticals and personal care products in water treatment using carbonaceous-TiO₂ composites: a critical review of recent literature," *Water Research*, vol. 142, pp. 26–45, 2018.
- [3] H. Cheng, J. Wu, F. Tian et al., "Visible-light photocatalytic oxidation of gas-phase Hg⁰ by colored TiO₂ nanoparticle-sensitized Bi₅O₇I nanorods: enhanced interfacial charge transfer based on heterojunction," *Chemical Engineering Journal*, vol. 360, pp. 951–963, 2019.
- [4] Y. Gai, J. Li, S.-S. Li, J.-B. Xia, and S.-H. Wei, "Design of narrow-gap TiO₂: a passivated codoping approach for enhanced photoelectrochemical activity," *Physical Review Letters*, vol. 102, no. 3, pp. 036402–036402, 2009.
- [5] Y. Zhang, L. Li, and H. Liu, "Photocatalytic Reduction Activity of Codoped with F and Fe under Visible Light for Bromate Removal," *Journal of Nanomaterials*, vol. 2016, Article ID 5646175, 7 pages, 2016.
- [6] Y. Zhang, L. Li, H. Liu, and T. Lu, "Graphene oxide and F codoped TiO₂ with (0 0 1) facets for the photocatalytic reduction of bromate: Synthesis, characterization and reactivity," *Chemical Engineering Journal*, vol. 307, pp. 860–867, 2017.
- [7] J. Kashyap, S. M. Ashraf, and U. Riaz, "Highly efficient photocatalytic degradation of amido black 10B dye using polycarbazole-decorated TiO₂ nanohybrids," *ACS Omega*, vol. 2, no. 11, pp. 8354–8365, 2017.
- [8] B. Petrie, R. Barden, and B. Kasprzyk-Hordern, "A review on emerging contaminants in wastewaters and the environment: current knowledge, understudied areas and recommendations for future monitoring," *Water Research*, vol. 72, pp. 3–27, 2015.
- [9] R. Loos, R. Carvalho, D. C. António et al., "EU-wide monitoring survey on emerging polar organic contaminants in wastewater treatment plant effluents," *Water Research*, vol. 47, no. 17, pp. 6475–6487, 2013.
- [10] M. Gavrilescu, K. Demnerová, J. Aamand, S. Agathos, and F. Fava, "Emerging pollutants in the environment: present and future challenges in biomonitoring, ecological risks and bioremediation," *New Biotechnology*, vol. 32, no. 1, pp. 147–156, 2015.
- [11] S. D. Richardson and S. Y. Kimura, "Water analysis: emerging contaminants and current issues," *Analytical Chemistry*, vol. 88, no. 1, pp. 546–582, 2015.
- [12] L. Jothinathan and J. Hu, "Kinetic evaluation of graphene oxide based heterogenous catalytic ozonation for the removal of ibuprofen," *Water Research*, vol. 134, pp. 63–73, 2018.
- [13] P. Chen, W. Lv, Z. Chen et al., "Phototransformation of mefenamic acid induced by nitrite ions in water: mechanism, toxicity, and degradation pathways," *Environmental Science and Pollution Research International*, vol. 22, no. 16, pp. 12585–12596, 2015.
- [14] J. Niu, Y. Li, E. Shang, Z. Xu, and J. Liu, "Electrochemical oxidation of perfluorinated compounds in water," *Chemosphere*, vol. 146, pp. 526–538, 2016.
- [15] J. Yang, Z. Wen, X. Shen, J. Dai, Y. Li, and Y. Li, "A comparative study on the photocatalytic behavior of graphene-TiO₂ nanostructures: Effect of TiO₂ dimensionality on interfacial charge transfer," *Chemical Engineering Journal*, vol. 334, pp. 907–921, 2018.
- [16] J. Madhavan, F. Grieser, and M. Ashokkumar, "Combined advanced oxidation processes for the synergistic degradation of ibuprofen in aqueous environments," *Journal of Hazardous Materials*, vol. 178, no. 1-3, pp. 202–208, 2010.
- [17] N. Kashif and F. Ouyang, "Parameters effect on heterogeneous photocatalysed degradation of phenol in aqueous dispersion of TiO₂," *Journal of Environmental Sciences (China)*, vol. 21, no. 4, pp. 527–533, 2009.
- [18] M. Long, J. Brame, F. Qin, J. Bao, Q. Li, and P. J. J. Alvarez, "Phosphate Changes Effect of Humic Acids on TiO₂ Photocatalysis: From Inhibition to Mitigation of Electron-Hole Recombination," *Environmental Science & Technology*, vol. 51, no. 1, pp. 514–521, 2016.
- [19] L. Songtao, Y. Pinghe, Z. Ling, H. Huanbiao, and W. Xingrang, "Effects of anions and humic acid on the degradation of CTAB by UV/Fe³⁺ process," *Industrial Water Treatment*, vol. 30, pp. 52–54, 2010.
- [20] G. Liu, N. Zhang, and M. Zhang, "Photo-degradation kinetics of 4, 4'-dibromobiphenyl in aqueous solution," *Environmental Science & Technology*, vol. 35, pp. 92–95, 2012.
- [21] M. Zhan, X. Yan, H. Yang, and L. Kong, "Study on the effect of natural aquatic humic substances on the photodegradation of bisphenol A," *Journal of Environmental Sciences*, vol. 25, pp. 816–820, 2005.
- [22] S. Zhang, J. Chen, X. Qiao, L. Ge, X. Cai, and G. Na, "Quantum chemical investigation and experimental verification on the aquatic photochemistry of the sunscreen 2-phenylbenzimidazole-5-sulfonic acid," *Environmental Science & Technology*, vol. 44, no. 19, pp. 7484–7490, 2010.
- [23] T. E. Doll and F. H. Frimmel, "Fate of pharmaceuticals—photodegradation by simulated solar UV-light," *Chemosphere*, vol. 52, no. 10, pp. 1757–1769, 2003.
- [24] S. Chen, Y. Hu, X. Jiang, S. Meng, and X. Fu, "Fabrication and characterization of novel Z-scheme photocatalyst WO₃/g-C₃N₄ with high efficient visible light photocatalytic activity," *Materials Chemistry and Physics*, vol. 149-150, pp. 512–521, 2015.
- [25] Y. Fu, X. Gao, J. Geng, S. Li, G. Wu, and H. Ren, "Degradation of three nonsteroidal anti-inflammatory drugs by UV/persulfate: degradation mechanisms, efficiency in effluents disposal," *Chemical Engineering Journal*, vol. 356, pp. 1032–1041, 2019.
- [26] L. Zhou, W. Song, Z. Chen, and G. Yin, "Degradation of organic pollutants in wastewater by bicarbonate-activated hydrogen peroxide with a supported cobalt catalyst," *Environmental Science & Technology*, vol. 47, no. 8, pp. 3833–3839, 2013.
- [27] B. Zhou and C. Chen, "Photosensitization of superoxide radicals by cyanine dyes," *Chinese Journal of Magnetic Resonance*, vol. 11, pp. 353–359, 1994.
- [28] C. E. Diaz-Urbe, M. C. Daza, F. Martínez, E. A. Páez-Mozo, C. L. B. Guedes, and E. Di Mauro, "Visible light superoxide radical anion generation by tetra(4-carboxyphenyl)porphyrin/TiO₂: EPR characterization," *Journal of Photochemistry and Photobiology A: Chemistry*, vol. 215, no. 2-3, pp. 172–178, 2010.